*Eur. J. Mech. B/Fluids 18 (1999) 675–692*


# Laminar separation on a forward facing step

H. Stüer *, A. Gyr, W. Kinzelbach

*Institute of Hydromechanics and Water Resources Management, Swiss Federal Institute of Technology, CH-8093 Zürich, Switzerland*

(Received 24 March 1998; revised 28 September 1998; accepted 22 October 1998)

**Abstract** – The separation ahead of a forward facing step was investigated under laminar flow conditions using the hydrogen bubble technique to visualise and PTV to evaluate the 3-D velocity field in an Eulerian representation in the vicinity of the step. Short-time averaged velocity fields allowed the construction of streamlines showing that the separation is topologically of an open bubble type with a span-wise quasi periodicity. The entrained fluid is continuously released by the front vortex which breaks out of the separation bubble in longitudinal streaks. The topology of this dynamic behaviour is described and confirmed by streamlines and vorticity lines. © Elsevier, Paris

## 1. Introduction

Separation is a phenomenon which appears under a variety of flow conditions and is encountered in many engineering problems. In the present study the laminar separation ahead of a forward facing step is investigated using the hydrogen bubble technique as a visualisation tool. In addition, Particle Tracking Velocimetry (PTV) was used to evaluate the 3-D flow field in Lagrangian and Eulerian form for a specific laminar flow rate. Laminar separation can be of a very complex three-dimensional nature and its understanding gives supplementary insight into turbulent separation for the same geometry, see Smith [1].

The configuration of a forward facing step has been investigated much less than its counterpart, the backward facing step. This is mainly due to the fact that the backward facing step is often used as a benchmark test for computations, whereas the calculation of the forward facing step is quite a delicate task [2]. In other words, very little has been published on the problem of the laminar separation on a forward facing step, and neither its topology nor its relevant scales are known in a predictable form. Although forward facing step configurations are used to enhance heat transfer rates and are often encountered in geophysical problems [3]. They also appear in flows over obstacles, such as buildings.

In the past, the three-dimensional behaviour of a separation was analysed by point measurements (LDA), two-dimensional techniques (PIV) or heat transfer measurements (IRSR). Alternatively, numerical simulations provided a fully resolved flow field for small Re-numbers and restricted geometries. Due to these restrictions and shortcomings, the main features of the separation phenomena have not been completely understood. Basically, measurements of the temporal 3-D flow field are needed to clarify the main topological structure. Of particular importance is the issue of whether the separation bubble in front of the step is closed or open. In other words, it is an open question whether fluid is entrained from the outer flow into the separation bubble due to a diffusion process or directly by a separation having a focus. In the former case, the separation bubble is two-dimensional and has an inner circulation described by closed streamlines (see *figure 1a*). In case of

* Correspondence and reprints

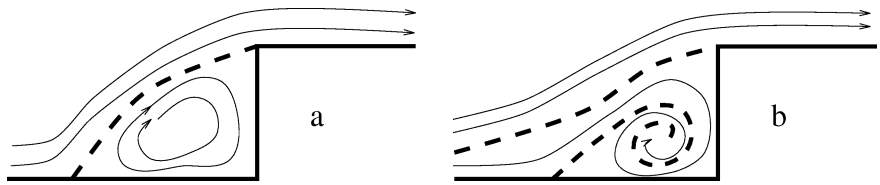


**Figure 1.** Sketch of a closed (a) and an open (b) separation bubble. The latter one shows that fluid is entrained and rolled up in a focus which has then to be released. Solid lines represent streamlines, dashed lines represent separatrix lines.

an open separation bubble, fluid is entrained between the two separatrices but due to continuity, it has to be released out of the separation bubble (see *figure 1b*). Separatrix stands for the analogy of a separation line in three dimensions and is defined by the separation surface. Three different mechanisms are possible:

- A two-dimensional vortex in span-wise direction grows in diameter due to the entrained fluid and is suddenly released as a blob.
- Another possibility is that the fluid is released at the corner where the step meets the sidewall and the flow has to match complex boundary conditions. This mechanism becomes dominant for narrow (width/height is of the order 1) channels. In our case with a large width/height ratio we could not observe a direct influence of the side walls, although a breakthrough at the side walls exists as can be seen in the right column of *figure 7*.
- The span-wise vortex becomes unstable and the fluid is released in the flow direction by vortices oriented in this direction. In this case the flow would be helical. It will be shown that this case is the main mechanism by which fluid is released out of the separation bubble, and it is this regime which has been investigated and commented on.

If this question could be resolved and supplemented by information on the three-dimensional flow field, it would then be possible to evaluate the amount of the entrained fluid and its residence time. This information is obviously important for predicting transport and reaction processes in the separation region, which cannot yet be adequately described by numerical simulations. The velocity values at the grid points of a three-dimensional grid have been evaluated by PTV and presented in the form of stream and vorticity lines. (If needed for numerical purposes the datasets can be obtained from the authors.)

The visualisation and measuring technique as well as the experimental setup are presented and discussed in Section 2. In Section 3 the results of the visualisation are shown. In addition, the interpolation technique for the Eulerian flow field is described, together with the data analysis achieved under certain restrictions, and images of streamlines as well as vorticity-lines are shown. The time resolution of the averaging process used is discussed in some detail to show the limitations of the present evaluation. As a result, the topology sketch of the Eulerian flow field is presented, together with a possible explanation of this particular separation process based on the evaluated stream- and vorticity-lines. In Section 4 the conclusions will be given.

## 2. Experimental setup, measurement and visualisation technique

To study separation phenomena it is necessary to obtain information on the whole flow field in the vicinity of the separation. To get a first impression of the flow structure, the hydrogen bubble technique was applied for different Re-numbers. To get a deeper insight into the flow structure and to obtain quantitative data, a PTV method was applied.

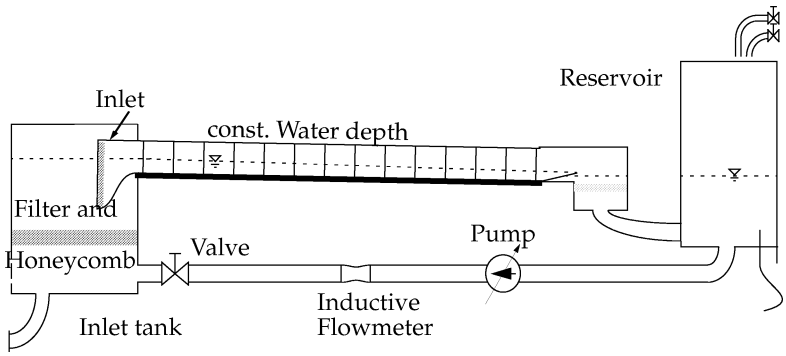


**Figure 2.** Overall sketch of the experimental facility. The details of the main test section is shown in *figure 5*.

### *2.1. Experimental setup*

The measurements were performed in an open water channel which is 24 m long and 0.6 m wide, for details see Virant [4]. Water is pumped in a closed circuit by a regulated radial pump and the throughput is controlled by a magneto-inductive flow-meter. The inlet has a shape to create an accelerated boundary layer and contains filters and flow conditioning devices to suppress perturbations, see *figure 2*. The main test section was 6 m long and located 15 m downstream of the inlet. It consisted of two 6000 mm $\times$ 600 mm $\times$ 8 mm glass plates, which formed the floor and the top of the channel. The top glass plate was supported by side-bars of Perspex, which had a cross section of 80 mm $\times$ 20 mm. This provided optical accessibility and very smooth channel walls. The cross section of the test area was 560 mm $\times$ 80 mm and the entry length was long enough to get a fully developed parabolic laminar velocity profile in the observation area. The upstream parabolic velocity profile was checked for perturbations by dye visualisation. The height of the step was 20 mm over the whole span. This gave a channel height to step height aspect ratio of $4:1$.

### *2.2. Hydrogen bubble visualisation technique*

To study flow structures the hydrogen bubble technique is widely used (see overview article Lian and Su [5]). A constant current source was connected to a wire (Cathode), which was mounted span-wise and parallel to the step within the recirculation zone as shown in *figure 3*, and to a thin copper plate (Anode) which was located 0.5 m downstream of the step. The copper wire was 0.1 mm in diameter and was tightly fixed over the hole span. When the channel is filled with water and a sufficient voltage is applied small hydrogen bubbles are generated at the wire. These small bubbles are convected by the flow and follow the local velocity, however with a small buoyancy contribution. It was tested by a zero flow rate experiment that the bubble rising velocity was much smaller than the convection velocity in the experiments. Since we are only interested in a qualitative picture of the flow structure, we neglect the buoyancy of the bubbles and assume that they follow the flow field sufficiently well within the observation volume.

With a photo-camera positioned directly above the step, pictures of the whole cross-section were taken. Furthermore, a CCD camera facing the step at an angle of 50° was placed alternatively in the middle, and near the right sidewall of the channel (see *figure 3*).

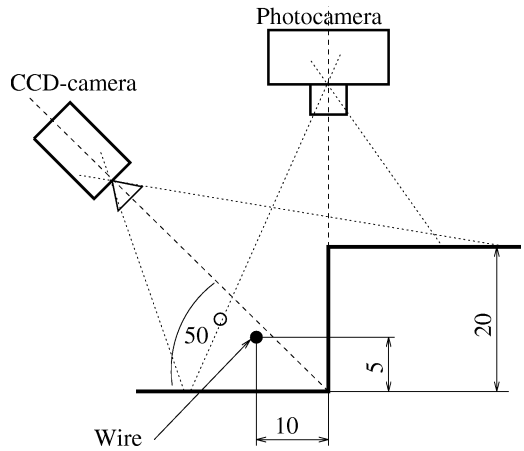


**Figure 3.** Sketch of the wire location and position of CCD camera and photo-camera (dimensions in mm).

### *2.3. PTV measuring technique*

The PTV technique used was developed at ETH Zürich and is suited to investigate laminar and turbulent flow problems [4]. The PTV setup is in principle the same as described in detail by Virant [4] and Dracos [6]. The flow was seeded with flow markers (Vestosint) which have a density of $1.02 \cdot 10^{-3}$g/mm$^3$ and a diameter of 40–63 $\mu$m. The observation volume was illuminated by two 400 W halogen-short-arc lamps. The motion of the flow markers was recorded by four 25 Hz CCD cameras (CCIR Sony XC77), which were focused on a rectangular volume, and stored on four U-matic tape recorders. After the experiment a sequence of 900 images was digitised and stored on hard disk. A sketch of the imaging chain is shown in *figure 4*.

After digitisation and calibration of photogrammetric parameters a program calculated the coordinates for up to 1300 particles in the observation volume (for details of the photogrammetric principles see [7,8]. Then a tracking procedure [9] was applied to connect the coordinates of the same particle in consecutive time steps. The velocity for each time step and trajectory can be calculated using a second order finite difference scheme.

In this study the observation volume was $60 \times 30 \times 64$ mm$^3$ and located at the centre of the channel. The bottom of the measuring volume coincided with the floor of the channel. The camera arrangement and the dimensions and location of the observation volume are shown in *figure 5*.

## 3. Data analysis

### *3.1. Visualisation*

*Figures 6* and *7* show some snapshots of the flow field for different Re-numbers. In *figure 6* the whole width of the channel is shown whereas in *figure 7*, in the left column, the middle part of the channel is shown and, in the right column, the flow near the right wall of the channel. These pictures give an impression of the typical flow structure of this particular separation phenomenon. The fluid inside the separation bubble is transported parallel to the step and released in streaks over the step. These streaks show a very definite periodicity as shown in *figure 6* where an overview of the whole span of 560 mm is given. A more detailed study of the breakthrough is reproduced for all Re-numbers tested in *figure 7*. These streaks, however are not steady and move slowly in the span-wise direction in an uncorrelated fashion. With increasing Re-number the transverse movement of the

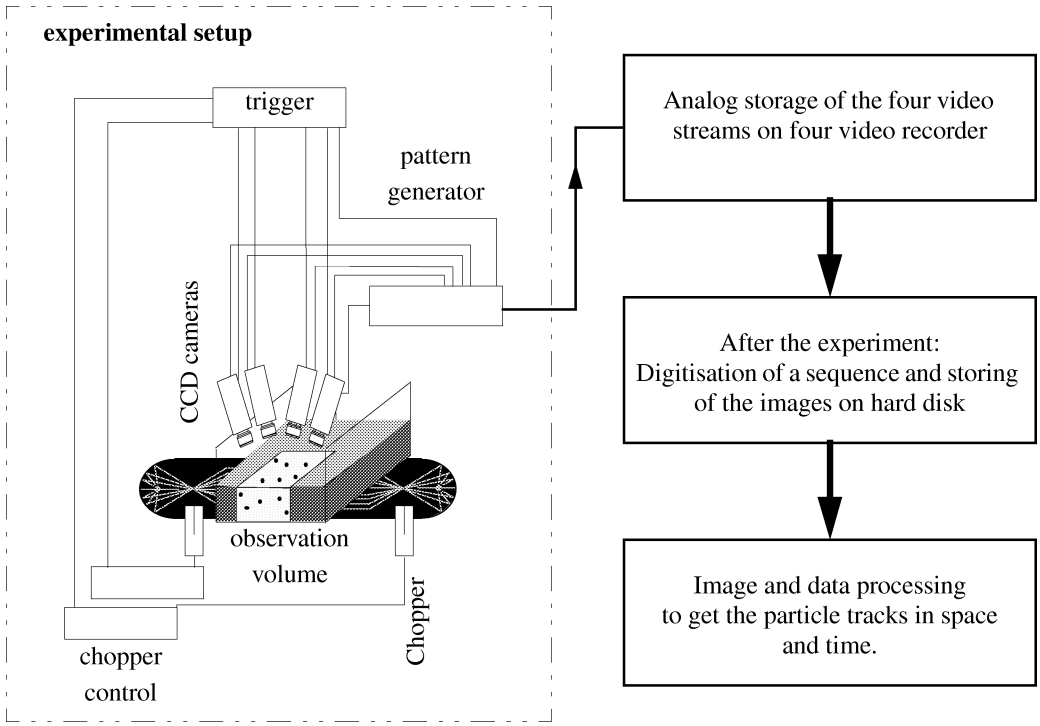


**Figure 4.** Flow chart of imaging chain.

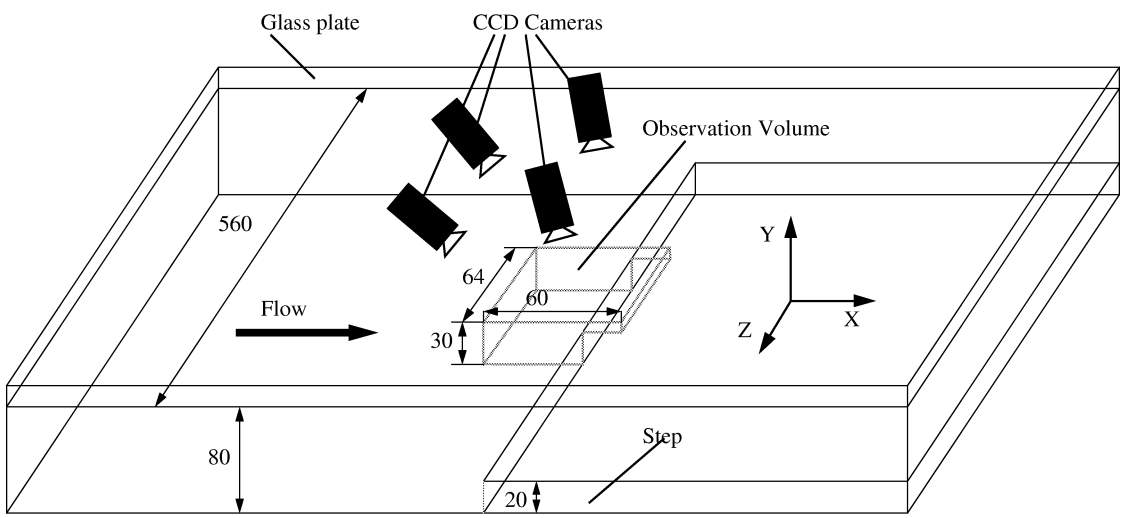


**Figure 5.** Flow channel with observation volume.

streaks becomes faster. Sometimes two streaks come close together and form one streak or if two streaks are far apart a new one in the middle is spontaneously generated. It seems that the side-walls have no effect on the unsteady behaviour. At least this effect is not supported by the visualisations (e.g. the side-walls could generate a steady disturbance wave where its vertices would be the origin of steady longitudinal vortex break-throughs). In addition the qualitative behaviour of the streak pattern remained the same for all Re-numbers tested.

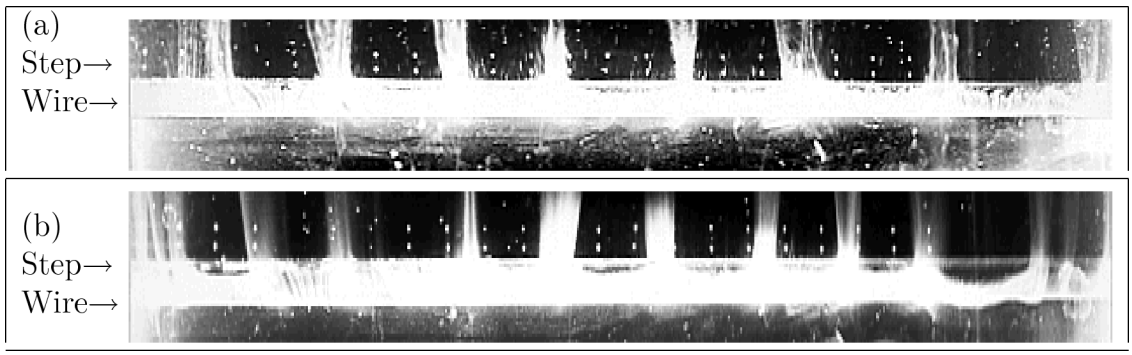


**Figure 6.** Hydrogen bubbles visualisation. The complete span is shown for two different Re-numbers: (a) Re 960, (b) Re 2300. Flow from bottom to top.

Visual observation at the highest Re-number (Re 8400, *figure 7g*) show the characteristics of a turbulent flow, whereas *figures 7g* and *f* display the transitional state and *figures 7a–d* belong to a laminar flow field. Despite these rather different flow states the main flow pattern remained the same. Note that the transition to turbulence is delayed due to the very smooth channel walls and a disturbance-free inlet. In addition, if one scales the Re-number with the channel height instead of the hydraulic diameter, one gets a 43% smaller Re-number.

### *3.2. PTV measurements*

Based on the visualisations we assumed that the main mechanism of the separation for the different Re-numbers investigated is the same. Hence, we used the PTV measurements only at one particular Re-number for which the technique was best suited. This was for our setup conditions at a Re-number of 2300 with respect to the hydraulic diameter of the upstream flow and a mean velocity $U_{\mathrm{m}}$ of 16.7 mm/s (or of a Re-number of 330, respectively, using the step height as the relevant length scale).

It is obvious that the more time resolved the measurements are the more informative they are. The present PTV method of measuring and evaluating the three-dimensional flow field is still very restricted in this respect because the temporal resolution of our system is relatively low with a frame rate of 25 Hz, thus limiting the PTV measurements to low velocities. The flow field which can be evaluated at one time-step is also limited by the maximum seeding density used in the observation volume. In the present experiment the mean distance of velocity vectors was too large over the volume to give a sufficient reconstruction of the flow field at each time-step.

A spatially uniform Eulerian velocity vector field was found by interpolating the randomly distributed velocity vectors with a Gaussian weighting function to the nearest grid point of a regular mesh [10]. The smallest finite grid size, given by the Nyquist criterion, is at least twice the average particle distance $\delta$

$$\delta = \left(\frac{V}{n}\right)^{1/3} \tag{1}$$

where $V$ is the observation volume and $n$ is the number of velocity vectors within $V$. Because these vectors are randomly distributed, the grid size must be even larger than estimated by this criterion. In our observation volume we could determine around 700 vectors at each time step. This would lead to a small number of control volumes and as a consequence to a small spatial resolution. To increase the spatial resolution, we superimposed consecutive instantaneous vector fields by using an ensemble average. This is justified as long as the flow field

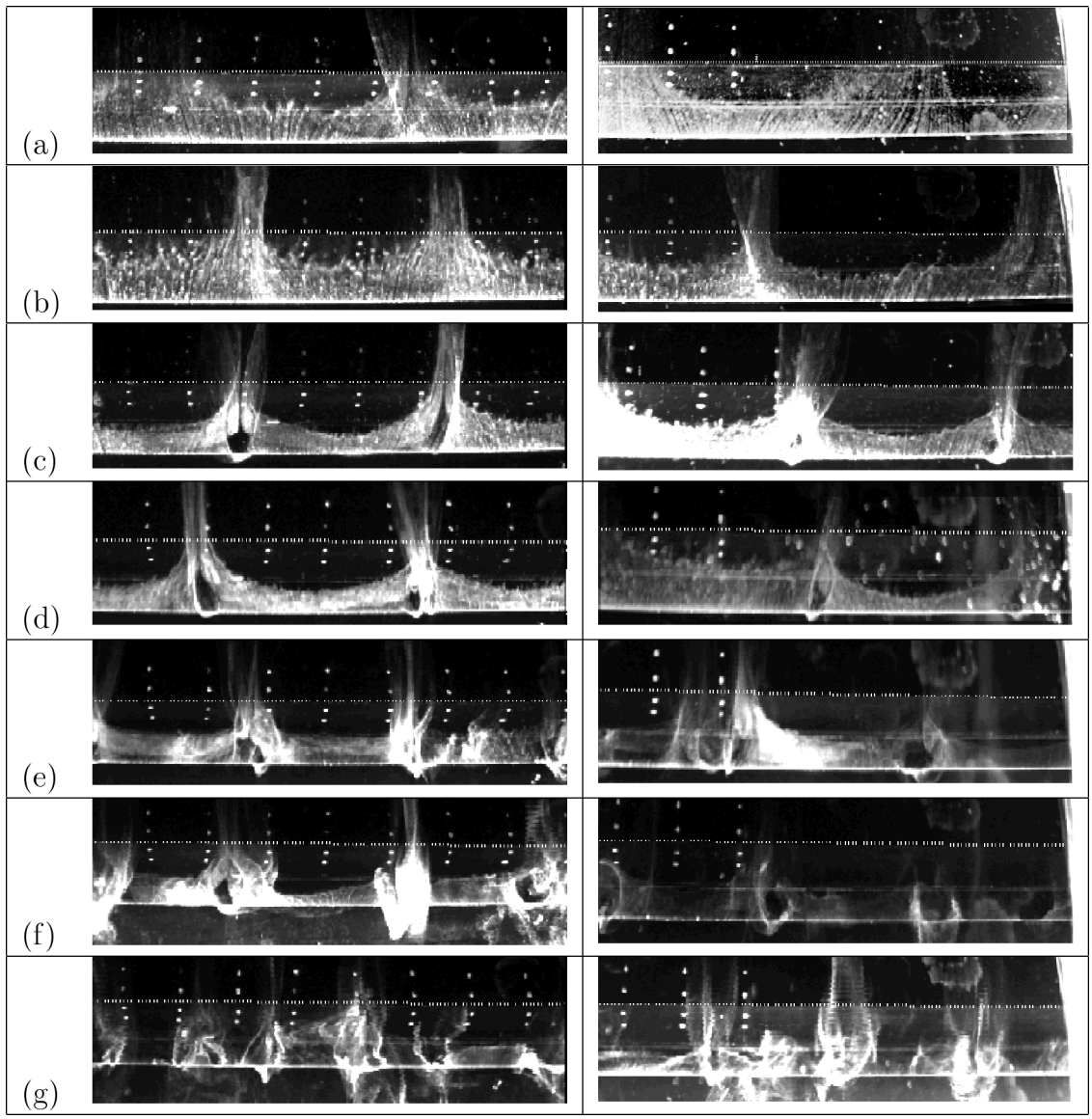


**Figure 7.** Hydrogen bubbles visualisation for different Re-numbers: (a) Re 940, (b) Re 1150, (c) Re 2300, (d) Re 3120, (e) Re 4600, (f) Re 6200 and (g) Re 8400. Flow from bottom to top. The left column shows about 160 mm of the middle part of the channel and the right column shows about 150 mm of the right side with the right wall of the channel. The dotted line gives the location of the edge of the step.

is quasi steady during such a time period. The large structures do not change significantly in size and their topology therefore remains unchanged.

We found an optimum between spatial resolution and characteristic time scale for an ensemble average of 6 s (150 frames). At an overall measuring time of 36 s, this leads to 6 ensemble averaged sequences. This procedure acts like a low pass filter and so it can only be expected to describe the large scale flow structure with limited accuracy. Although this is a severe restriction, the results could be used to give an answer to the questions posed in the introduction.

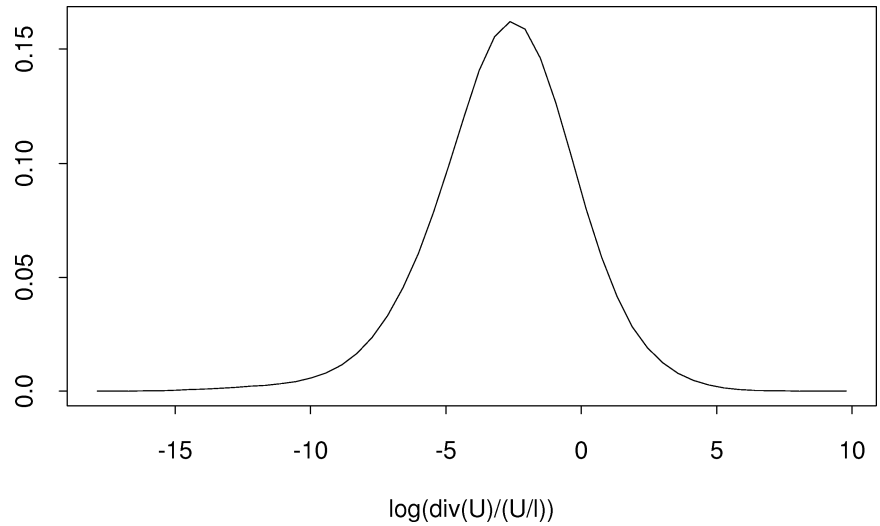


(a)

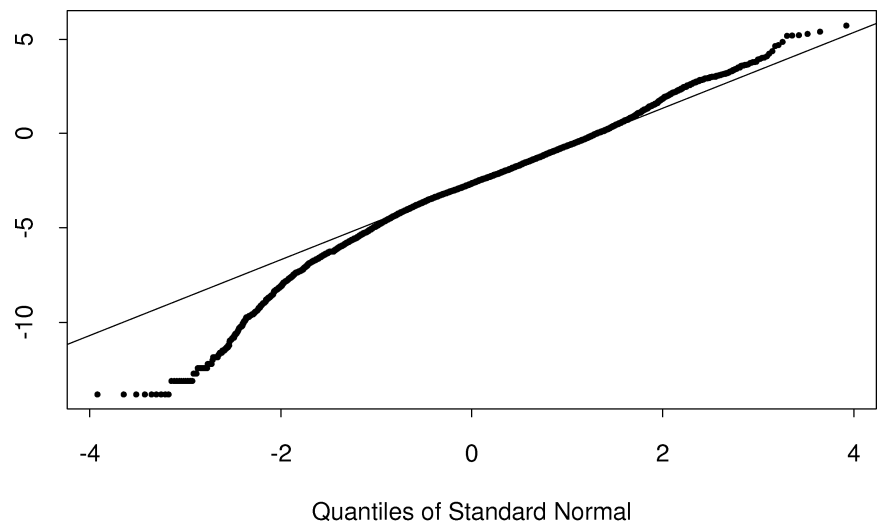


(b)

**Figure 8.** (a) Distribution of the error-estimator based on Eq. (2) for one short-time averaged sequence. The ordinate represents the number of control volumes normalised to 1. (b) Normal probability plot of the top plot. The fitted line shows a Gaussian distribution. The greater spread of the extreme quantiles for the data is indicative of a long-tailed distribution.

The resulting 12 160 control volumes consisted of cubes of 2 mm length. The interpolation technique was tested with respect to the following assumption

$$|\nabla \cdot u_i| \ll \frac{|u_i|}{\ell} \tag{2}$$

where $u_i$ is the velocity vector for each control volume $i$, and $\ell$ is a characteristic length scale (e.g. cube length). This is an error estimate of how well the continuity equation is satisfied, if the divergence is calculated for each

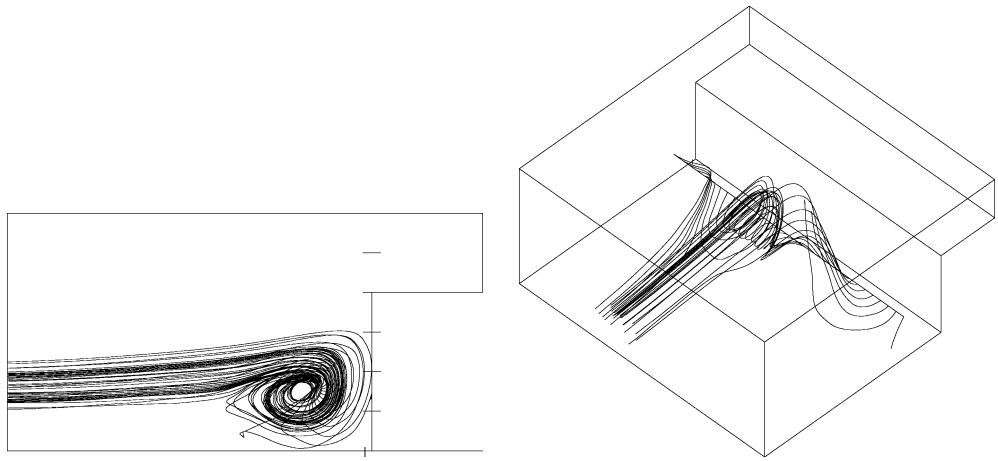


**Figure 9.** Streamlines calculated backwards from a line probe placed parallel to the step.

control volume and given as a fraction of the right hand side of Eq. (2). As an example, a log distribution of the error-estimator (Eq. (2)) and its normal probability plot for one short-time averaged sequence are shown in *figure 8*. It can be seen that the error is log-normally distributed (except at the tails). The mean value of the error-estimator is about 6% for each ensemble averaged sequence. From this we conclude that the method is suited to investigate laminar separation problems.

From the short-time-mean Eulerian velocity fields, streamlines and vorticity-lines as well as some basic topological aspects of the separation mechanism can be determined in a *large scale* approximation. With the Lagrangian representation, quantities like the mean residence time are in principle also accessible. Although quantities such as an estimate of the entrainment rate and the volume of the separation bubble as a function of time can be evaluated from the Eulerian representation if the position of the separatrix is known, the uncertainties encountered and poor spatial resolution, did not allow, however, their calculation.

### *3.2.1. Streamlines*

From the velocity vector fields the streamlines and vector plots can be calculated. This was done with the visualisation program AVS. We only show streamline images because they are more meaningful in visualising the flow-field in 3-D coordinates than vector cuts would be. The streamlines are generated at selected sample points. For every integration step, streamlines advance from each sample point through space, based on the interpolated value of the node vectors surrounding the point. The result is a set of streamlines showing the progress of massless particles moving under the influence of the vector field. These streamlines provide the basis for answering most questions related to a separation flow. Note that the visualisations and results in this and the following subsection were calculated for the observation volume shown in *figure 5*.

In *figure 9a* the side view of streamlines, and in *figure 9b* the bird's eye view of the same streamlines are shown over an area corresponding approximately to one "periodic" length scale in span of an open separation bubble, which has in the present case a length of about three step heights. At the stagnation point, the pressure field accelerates the fluid sidewise until it is released over the step. The complex surfaces spanned by the separatrices can be imagined from *figure 10* where sample points were placed in a plane in front of the step and streamlines were calculated backwards in space.

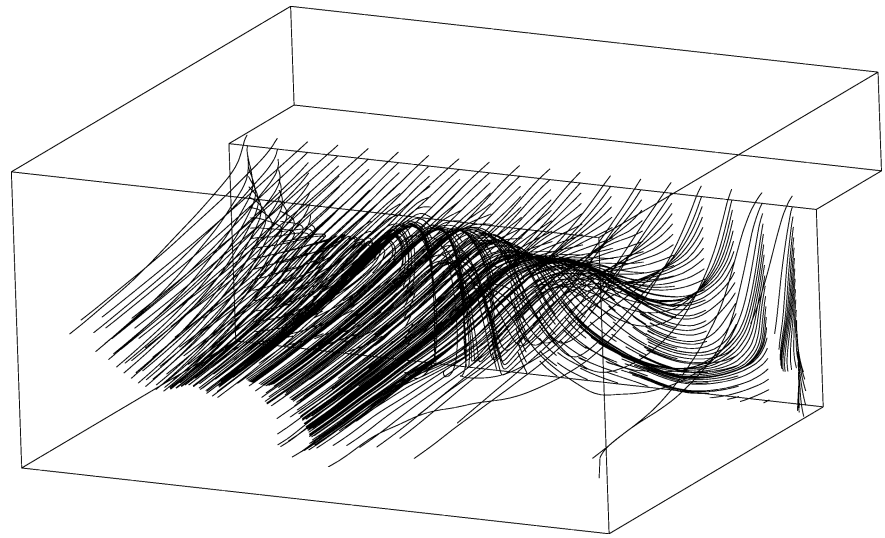

**Figure 10.** Streamlines showing the complex surfaces of the separatrices.

The separation bubble consists of fluid entering the bubble as sketched in *figure 1b*. The entrained fluid accumulates over the whole bubble span and gets concentrated in a focus that is identical to the helical vortex core through which the fluid is transported sideways until it is continuously released over the step. The fluid collected in this vortex turns over only a few times until it is released (i.e. after a rather short residence time).

However, the bubble is by no means steady. It changes position and shape at a large time scale, but any quantification would need a longer measurement time and also a larger observation volume than was used in this experiment. To elucidate the dynamics of the separation bubble, "wall-streamlines", streamlines close to the wall (at a distance less than a grid size), were evaluated and represented in *figure 11* for the six consecutive short-time averaged periods. These wall-streamlines are equivalent to pictures found by the oil-streak technique, because the motion of the particles close to the wall is in the direction of the local maximum shear stress. These wall-streamlines have the advantage of showing a much more instantaneous picture than the oil-streak technique would do.

*Figure 11* shows that a separation bubble travels parallel to the step and another bigger one moves into the observation area. The separation line of the larger bubble is almost three times further away from the step than the separation line of the smaller one. The bigger bubble deforms the smaller one slightly, but the topological patterns of both do not change.

The bifurcating character of the central streamlines is shown in *figure 12*, where streamlines of two line-probes are located on each side of the "plane of symmetry". This bifurcating character is even more pronounced in *figure 13* where the streamlines of two neighbouring sample points were calculated. It also shows the helical character within the separation bubble.

To get an impression of the velocity within the separation we made a line probe sample parallel to the step and calculated the velocity components along this line, see *figure 14*. The line probe was placed 7.5 mm in front of the step and 7.5 mm from the bottom (roughly the position of the line probe in *figure 9b*) and mainly within the core of the separation bubble. The dataset used was the first one (0–6 s) corresponding to *figure 11a*.

Note that the core of the separation bubble is bent and that the velocity in the $x$ and $y$ directions is not zero everywhere along the straight line sample. The important result of *figure 14* is that the span-wise velocity component is relatively large, almost $1/4$, in magnitude, of the mean upstream velocity ($U_{\mathrm{m}} = 16.7$ mm/s).

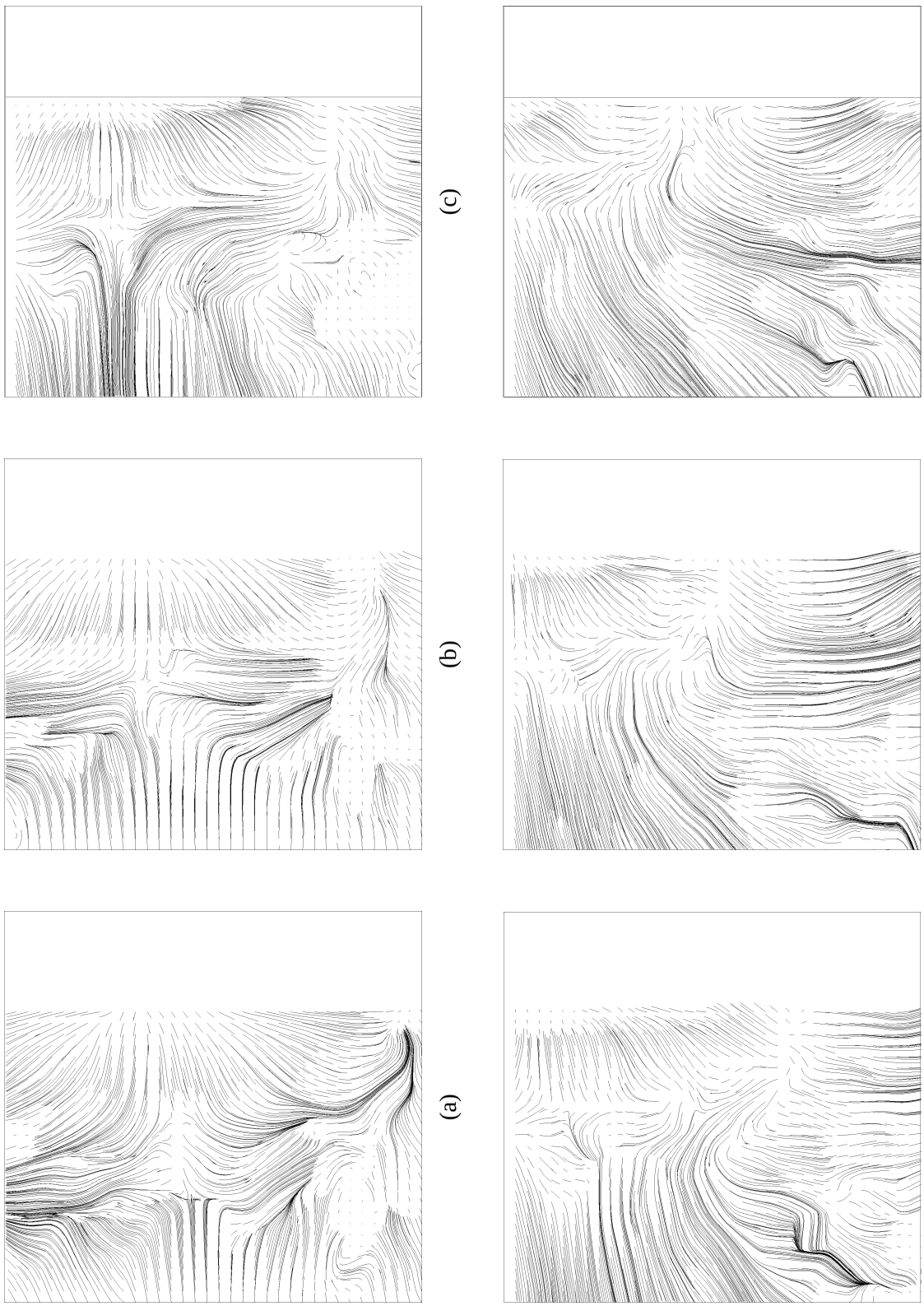


Figure 11. "Oil-streak" consecutive images for Re 2300 in front of the step. Each image is sampled over 6 s. (a) 0–6 s, (b) 6–12 s, (c) 12–18 s, (d) 18–24 s, (e) 24–30 s, (f) 30–36 s. Flow from left to right.

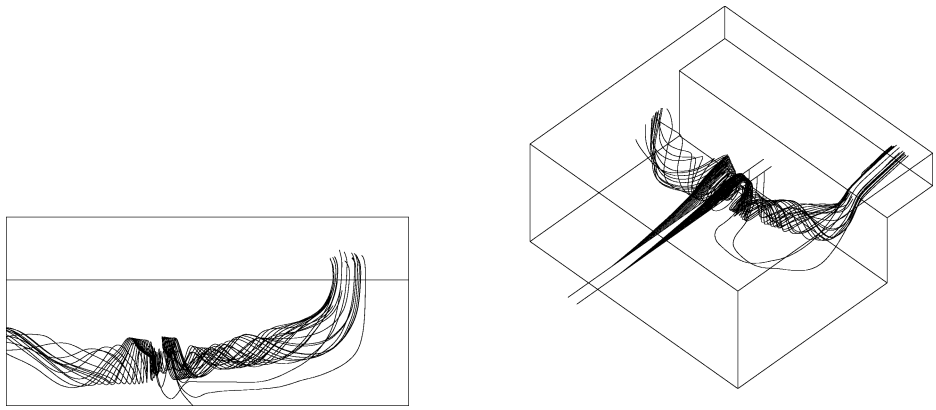

**Figure 12.** Streamlines calculated for two line probes. Same image different view.

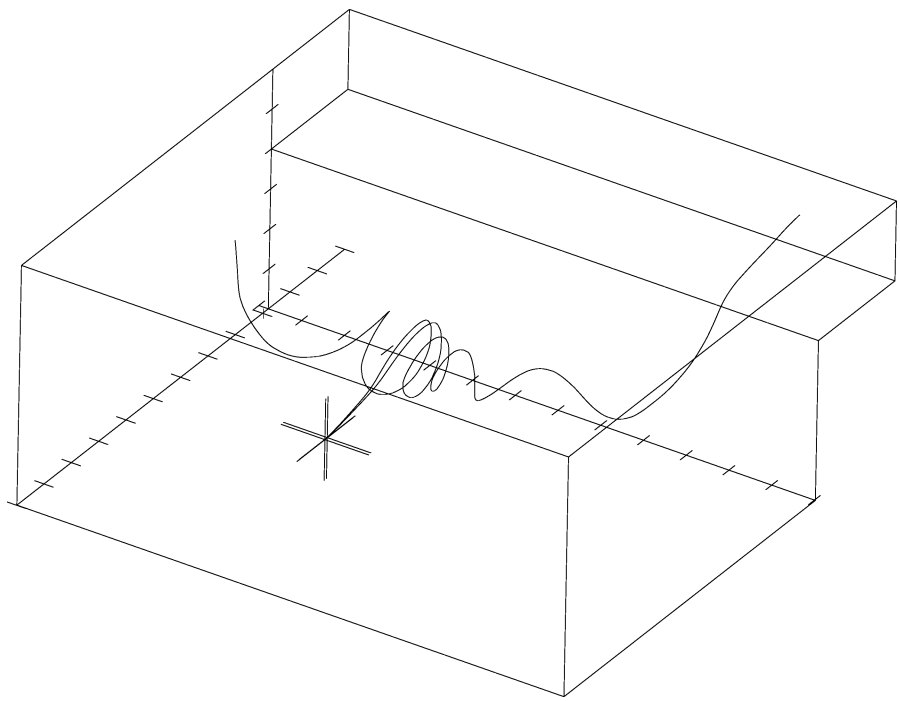

**Figure 13.** Streamlines calculated for two sample points (indicated by the two crosses) close together.

### *3.2.2. Vorticity-lines*

The vorticity-lines were constructed with the same algorithm as the streamlines by using the vorticity vectors at the grid nodes. The vorticity vectors were constructed from the spatial derivatives of the short-time-mean velocity field with a second-order scheme and are shown in *figure 15*.

The vorticity lines are concentrated in front of the step as expected in a front vortex with span-wise vorticity. Since the streamlines have the same orientation it is confirmed that the flow is helical. In the area of "break-through", the vorticity-lines tend to line-up in the stream-wise direction as the streamlines do. Thus the flow

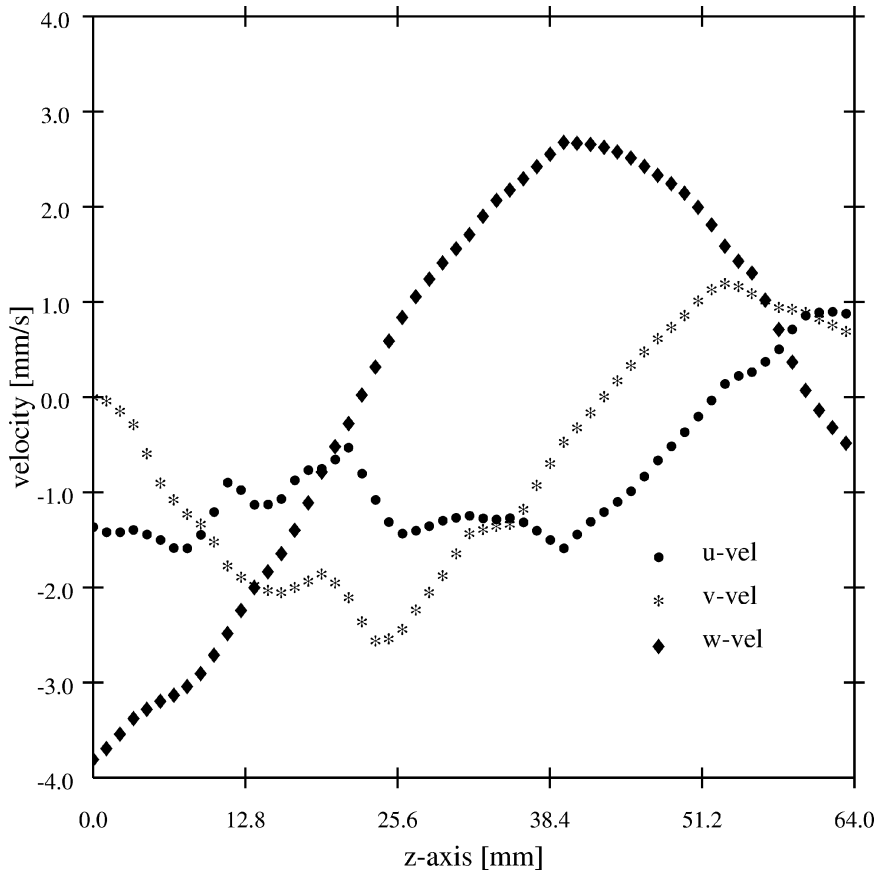


**Figure 14.** Velocity components along a line probe placed 7.5 mm in front of the step and 7.5 mm from the bottom parallel to the step.

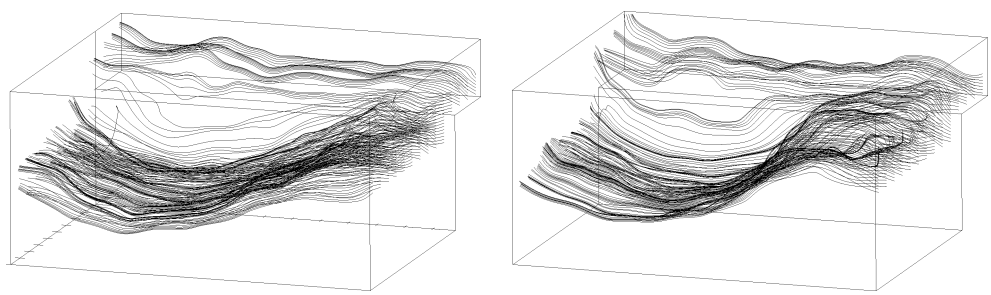


**Figure 15.** Large scale vorticity lines (6 s difference).

remains there mainly helical and the flux of fluid is concentrated in a vortex. On the step an astonishingly rapid dispersion and reorientation of the transported vorticity occurs. This means that the new vorticity generated on the step is much larger than the transported vorticity.

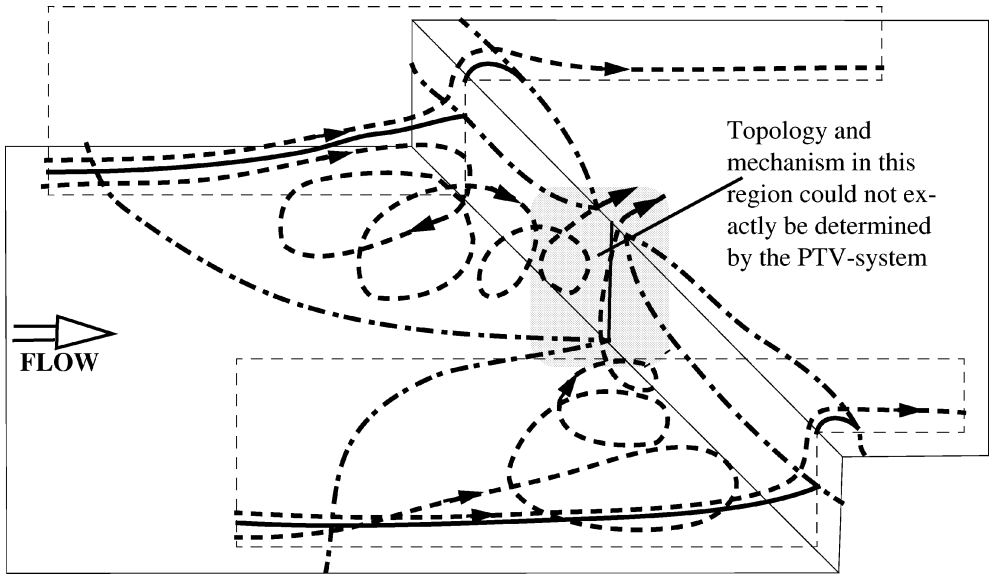


**Figure 16.** Topology of laminar separation on a forward facing step. Bold solid lines: separatrix, bold dashed line: streamlines, bold dashed dotted line: separation and reattachment lines. Note that in the span-wise direction the boundary condition is periodic.

*3.2.3. Basic topology of the separation*

The streamlines, which show the formation of the principal vortex, and also the main topology of the separation bubble can be constructed as sketched in *figure 16*. One of the most important elements of a topological description is the separatrix and its position.

First we assume that laminar separation bubbles at moderate Re-numbers are topologically open, that means two separatrices are present, the outer one coming from infinity and ending in a reattachment line which is a stagnation line at the step, and the other one from the separation line, and is rolled up in a focus. The main separatrix is the outer one which is the surface separating the region of fluid flowing into the separation from the one flowing around it.

Since the separatrices are formed by streamlines, they can be constructed from those, as long as we know the separation line or reattachment line. In our case these lines can in principle be found by placing a plane parallel and close (less than one grid size) to the bottom or the step. In these planes the projected velocity vectors should converge to the separation line or diverge from the reattachment line, but it is not a straightforward task to calculate these lines, primarily because the velocities close to a wall are small and the lines are curved as shown in *figure 16* or in *figure 11*, respectively. Furthermore, the spatial resolution was too low to construct meaningful separatrices, but they can be envisaged when considering the total field of streamlines.

The direct entrainment into the separation bubble, which is obtained by neglecting entrainment by diffusion through the outer separatrix, can be estimated as the fluid which flows beneath this separatrix and the bottom. It is this fluid which inflates the separation bubble and has to be released. The entrained fluid is released through longitudinal vortices. It is an open question how the flow organises itself in a topologically correct form and what the reason could be for the quasi periodic scale in span.

This scale must be the result of an instability process which is as yet unknown. In our view three possible mechanisms can be thought of:

- A wave in the vortex core which by self-induction becomes unstable:
  Conforming with this hypothesis would be the physical picture that the bending of the core at the side-

walls produces a self-induced disturbance wave which propagates on the vortex core. By reflection at the side-walls a defined wavelength is established and the vertices of this wave become the origin of longitudinal vortex break-through. In our experiments we could not find an influence of the sidewall on the behaviour of the central region of the main vortex in span.

- A vortex breakdown:
  A vortex breakdown could occur if by an instability of the helical flow, induced for example by the mass-transport, the entrained vorticity cannot be removed locally.
- An instability of Taylor–Görtler type, which is discussed in the following.

Based on the centrifugal instability as formulated by Rayleigh [11], curved streamlines produce longitudinal vortices on the concave side as shown by Görtler [12] for boundary layer flows, by Taylor [13] for Couette flows between concentric cylinders, and by Dean [14] for curved channels. The curvature in our case is due to a positive pressure gradient in the flow approaching the step. The boundary is formed by the wall up to the location where the inner separation occurs and follows the inner separatrix from there to the inflection point. This part would act like a curved surface producing Görtler instabilities, and the outer separatrix (dotted line in *figure 17*) also acts up to the inflection point in such a way.

Only when using several critical assumptions for the Taylor–Görtler geometry could the radius $R$ be related to the observed spacing of the longitudinal vortices. Longitudinal vortices in front of the separation have also been postulated by Pollard et al. [3] as necessary to reproduce their experimental results by a large eddy numerical simulation scheme. However, since the vorticity produced by this mechanism is rather minute, (i.e. we could not predict them from the streamline images and they must therefore be very weak or even non-existent), an additional experiment was performed to check the hypothesis.

About 100 mm in front of the step vortex, generators were placed which generated vorticity close to the bottom wall. The generated vortices were relatively strong, much stronger than any Taylor–Görtler vortices, (they could easily be visualised by the hydrogen bubble technique) so that they would have to dominate the instability process. Although the spacing between the vortex generators was varied, the vortex spacing and behaviour of the longitudinal vortices releasing the fluid out of the separation bubble remained almost the same, and we therefore conclude that a possible Taylor–Görtler instability cannot trigger the spacing of the streaky pattern. In other words, the instability of the separation bubble is of much higher inherent nature and the

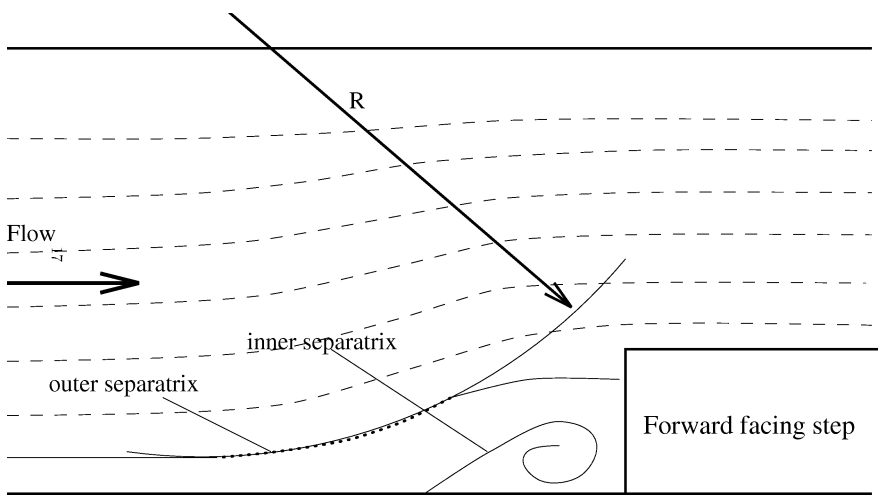


**Figure 17.** Principle sketch of the geometry in the flow region. $R$ is the radius of the outer boundary of the Taylor–Görtler geometry.

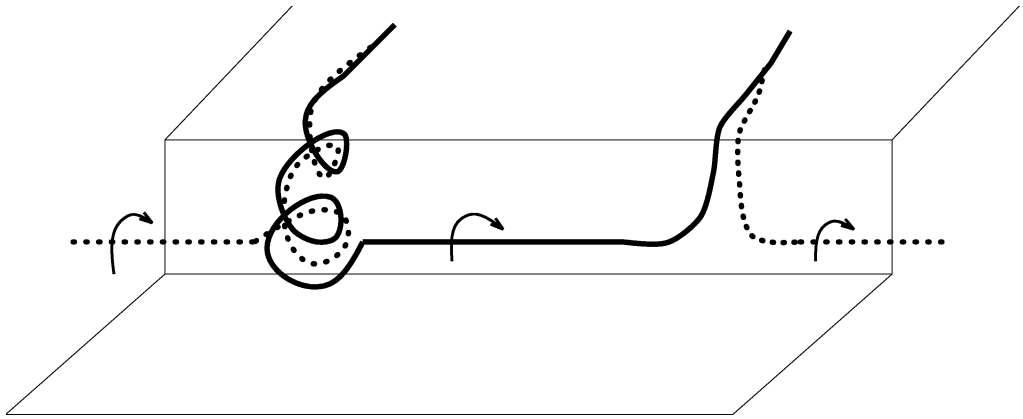

**Figure 18.** A sketch of the vortex interaction of two branches of the front vortex. Dotted and solid line: branches of the front vortex. Left side: Example for branches of different strength (exaggerated representation). Right side: Example for branches of comparable strength.

explanation of the quasi periodicity is a still unsolved problem, but we now know that some of the explanations usually given fail.

Whatever the cause of the instability, the observation allows a refinement of the topology in the area of breakthrough into two cases. Firstly, if the two branches on each side of the breakthrough are of comparable strength (e.g. *figure 7c* left column) they are lifted over the step as shown in *figure 18* on the right. Secondly, if one branch is much stronger than the other, the longitudinal vortices are formed by a loop of the front vortex, both side branches spiralling around each other and forming a single vortex, see *figure 18* on the left. The "oil-streak" patterns in *figure 11* can be interpreted as a foot print of the front vortex alternatively bent towards and away from the step. However, the longitudinal vortices created are rather weak compared with the newly created vorticity at the wall above the step and as this starts to dominate, the longitudinal vortices disappear, whereupon the vorticity becomes largely aligned with the span-wise direction again.

## 4. Discussion and conclusion

The laminar separation on a forward facing step was found to be an open three-dimensional separation bubble. The release of entrained fluid occurs continuously in longitudinal vortices at span distances with a quasi periodicity.

At decreasing Re-numbers we could recognise an increase of the distance between the breakthroughs in span and therefore one could speculate that the topology remains unchanged and the final situation would be that a single separation bubble remains with a release of fluid at its end where the step is bounded by the side walls. Whether at an even lower Re-number a closed separation bubble can appear remains an open question, because at much lower Re-numbers the particle tracking method fails at the moment when too many particles settle on the floor and cannot be moved by the flow any more.

The separation is unsteady and travels in transverse direction, slowly compared to the short-time-scale over which the field vectors have been averaged, but fast enough to be an important parameter describing the phenomenon. The scale of a separation unit in the span-wise direction was, however, too large for the observation field and therefore could not be quantified statistically.

An interesting result is that the quasi periodic spacing between the longitudinal vortices is an inherent value given by the flow geometry and which resisted even a strong forcing by vortex generators. Pollard et al. [3]

investigated the flow over a forward facing step experimentally and numerically. The relative dimensions and the Re-numbers of their experiment are comparable, with the exception that the aspect ratio of step height to channel height was larger ($h/H = 0.47$). They observed the same unsteady streaky patterns but with a smaller spacing, which would support a picture of Taylor–Görtler interaction. They concluded from their numerical simulation that the streak spacing is a result of a trigger mechanism by Taylor–Görtler like vortices which we can not support from our experiments.

For turbulent cases at Re-numbers of the order of $10^4$, Dimaczek et al. [15], using a crystal violet visualisation technique, observed a similar vortical behaviour of a flow over a square rib. They neither interpreted the quasi periodicity of the longitudinal vortices nor did they give a close topological view of the flow field, but they showed that the spacing in span is given in this case as 0.4–0.8 of the channel height. The existence of longitudinal vortices under turbulent flow conditions for this geometry was confirmed by large eddy simulations done by Werner and Wengle [16].

Another result to be debated is the observed independence of the flow field from the end wall corner eddies. This dependence is, on the one hand, often postulated and, on the other hand, neglected when one assumes two-dimensionality. It is evident that for narrow channels they become dominant; but is the spacing of the longitudinal vortices also a function of the wall? In our case, where we have a width of 28 step heights, no interaction of the central part of the flow with the one at the wall was observed. Freitas and Street [17] investigated a flow in a square cavity with an aspect ratio of length to width of 3. They found that the laminar flow in such a cavity can be described by a complex vortex system releasing fluid to the outer flow in longitudinal vortices with a time variant spacing. They came to the conclusion that the span-wise instability is of Taylor–Görtler type, but also a clear interaction with the end wall corner eddies was seen. Their flow was extremely confined but of a comparable geometry so that we cannot exclude small disturbances generated at the end walls being the source of the chaotic behaviour of the releasing process.

## Acknowledgements

The authors thank the Swiss National Science Foundation for providing the research grant for the present study (Grant No.2-77-240-96) and acknowledge the suggestions made by the members of IFD ETHZ. H.S. would also like to thank Stefan Blaser for fruitful discussions and a critical reading of the manuscript.

## References

[1] Smith F.T., Steady and unsteady boundary layer separation, Ann. Rev. Fluid Mech. 18 (1996) 197–220.
[2] Friedrich R., private communication, 1997.
[3] Pollard A., WaKarani N., Shaw J., Genesis and morphology of erosional shapes associated with turbulent flow over a forward-facing step, in: Ashworth P.J. et al. (Eds), Coherent Flow Structures in Open Channels, Wiley, Chichester, 1996, pp. 249–265.
[4] Virant M., Anwendung des dreidimensionalen Particle-Tracking-Velocimetry auf die Untersuchung von Dispersionsvorgängen in Kanalströmungen, Dissertation, Nr. 11678, ETH Zürich, 1996.
[5] Lian Q.X., Su T.-C., The Applications of the Hydrogen Bubble Method in the Investigations of Complex Flows, Atlas of Visualization II edited by The Visualization Society of Japan, CRC Press, Boca Raton, FL, 1996.
[6] Dracos T. (Ed.), Three-Dimensional Velocity and Vorticity Measuring and Image Analysis Techniques, ERCOFTAC Series Vol. 4, Kluwer Academic, Dordrecht, 1996.
[7] Maas H.-G., Digitale Photogrammetrie in der dreidimensionalen Strömungsmesstechnik, Dissertation, Nr. 9665, ETH Zürich, 1992.
[8] Maas H.-G., Grün A., Papantoniu D., Particle tracking in three-dimensional turbulent flows. Part I: Photogrammetric determination of particle coordinates, Exp. Fluids 15 (1993) 133–146.
[9] Malik N., Dracos T., Papantoniu D., Particle tracking in three-dimensional turbulent flows. Part II: Particle tracking, Exp. Fluids 15 (1993) 279–294.
[10] Agüí J.C., Jiménez J., On the performance of particle tracking, J. Fluid Mech. 185 (1987) 447–468.

[11] Lord Rayleigh, On the dynamics of revolving fluids, Scientific Papers, 6, Cambridge University Press, 1916, pp. 447–453.
[12] Görtler H., Über den Einfluss der Wandkrümmung auf die Entstehung der Turbulenz, ZAMM 20 (1940) 138–147.
[13] Taylor G.I., Stability of a viscous liquid contained between two rotating cylinders, Philos. Trans. Roy. Soc. London Ser. A 223 (1923) 289–343.
[14] Dean W.R., Fluid motion in curved channel, Proc. Roy. Soc. A 121 (1928) 402–420.
[15] Dimaczek G., Kessler R., Martinuzzi R., Tropea C., The flow over two-dimensional surface mounted obstacles at high Reynolds numbers, in: 7th Symp. Turb. Shear Flows, Stanford University, Stanford, 1989, pp. 10.1.1–10.1.6.
[16] Werner H., Wengle H., Large eddy simulation of turbulent flow over a square rib in a channel, in: Fernholz H.H., Fiedler H.E. (Eds), Advances in Turbulence, 2, Springer, Berlin, 1989, pp. 418–423.
[17] Freitas C.J., Street R.L., Non-linear transient phenomena in a complex recirculation flow: A numerical investigation, Int. J. Num. Meth. Fl. 8 (1988) 2807–2815.